

A 2MW direct drive wind turbine; vector control and direct torque control techniques comparison

Mehdi Allagui

OthmanBk Hasnaoui

Jamel Belhadj

High Engineering School of Tunis; Electrical Systems Laboratory, Tunis, Tunisia

Abstract

This paper presents a comparative study on the most popular control strategies used to control high power, Direct Drive Wind Turbines. The studied wind turbine is equipped with a supervision scheme in order to fulfil Grid connection requirements (GCR). For the generator-side converter, performances of the Field Oriented Control (FOC) and Direct Torque Control (DTC) are compared. Concerning the grid-side converter, Voltage Oriented Control (VOC) and Direct Power Control (DPC) are examined. The comparison is based on various criteria mainly, steady-state and transient performances. In addition, performances are evaluated in terms of low voltage ride through capabilities (LVRT), power limitation and reactive power control. It has been shown that best power quality features are given by vector control techniques. On the other hand, direct control offers the better dynamic response and power cross-coupling is substantially lower. Furthermore, during fault, the wind turbine does not trip for both techniques. However, vector control is better since it gives low power oscillations.

Keywords: Direct Drive, FOC, DTC, VOC, DPC, supervisory control

1. Introduction

Wind energy is a promising alternative to traditional energy sources (The European Wind Energy Association, 2010). Due to increasing wind power penetration, the improvement of control strategies

becomes a major challenge for manufacturers in order to comply with the grid connection requirements (Gabriele, 2008). Consequently, new wind power plants are increasingly expected to provide ancillary services which maintain reliable operation of the interconnected transmission systems (Lov *et al.*, 2007; Heier, 2006). Compared to other wind turbine technologies (Muni Prakash *et al.*, 2012; Pena *et al.*, 1996), Direct Drive topology showed itself to be the most promising technique because it offers variable speed operation and fulfils GCR with high efficiency (Akhmatov, 2005).

The power electronics subsystem is composed of two voltage source inverters (VSI) separately controlled. Control strategies based on direct power and vector oriented control are investigated for normal and distorted operating conditions. Control techniques for the Permanent Magnets Synchronous Generator intend to control the torque and the flux. On the other hand, control strategies for the GSC intend to decouple the active and reactive power delivered to the grid. To achieve these objectives, vector control techniques require current control, in the rotating reference frame, and decoupling between the components so that the electromagnetic torque and power are indirectly controlled. In direct control strategies, the first step is to estimate torque and power. These two variables are then controlled directly, resulting in less complex and faster algorithms (Bin Wu *et al.*, 2011).

For both techniques the advanced controller part was not considered. However, they give very good control performance, but the performance study was not explored for a large wind farm connected to grid (Lather *et al.*, 2013).

Consequently, it is relevant to evaluate the per-

formance of vector and direct control techniques, in order to identify which is the most suitable large scale generation. Therefore, in this work, FOC and DTC control strategies for the generator-side converter and VOC and DPC for the grid-side converter are considered.

In the first section, the wind turbine model is presented. The second section presents the control strategies of the generator-side converter. Performances of the two control techniques are simulated and analysed. The third section presents the control strategies of the GSC with a comparative study. Finally, in the last section presents the developed supervision algorithm used to control reactive power. Transient stability of the wind system during grid faults are investigated for both control strategies.

2. Direct drive wind turbine model

The wind turbine consists of the following components: A three-bladed rotor with the corresponding pitch angle controller; the MPPT algorithm; a PMSG with two back-to-back power converters (Carlsson, 1998), a DC-Link capacitor, and a grid LC-filter. The control of the PMSG-WT consists of two parts, the generator side control and the grid side control. The scheme of the wind turbine system is shown in Figure 1.

3. Control strategies for the generator side converter

3.1 Field oriented control

FOC strategy is generally applied to the Generator-side converter (Figure 2). It allows controlling the rotor speed through the control of the electromagnetic torque. Torque control is achieved by setting

to zero the d component of current and the torque is controlled through the q component. Details of this control strategy for variable pitch wind turbine and the MPPT algorithm are presented in Allagui et al., (2013).

3.2 Direct torque control

The basic principle of DTC is to select proper voltage vectors using a pre-defined switching table (Rahman et al., 2003). Selection is based on hysteresis control of stator flux linkage and the torque. In which case, the stator flux and the torque are controlled independently and directly. The torque hysteresis comparator is a three valued comparator. Whereas that, the flux hysteresis comparator is a two valued comparator. The control scheme of DTC is developed as shown in Figure 3.

3.3 Comparative study of DTC and FOC control

In order to compare the dynamic behaviour of these control techniques, FOC and DTC responses are presented in Figure 4. Simulations have shown that the FOC has higher torque ripple than DTC technique. Electromagnetic torque oscillation is evaluated using the Total Waveform Oscillation (Two), given by:

$$T_{WO} = \frac{\sqrt{T_{em-rms}^2 - T_{em-dc}^2}}{|T_{em-dc}|} * 100\% \quad (1)$$

Where T_{em-rms} and T_{em-dc} stand for the electromagnetic torque rms and average values, respectively.

Steady-state simulations show that the best power quality features and the smaller power-tracking error are given by the VOC technique. On the

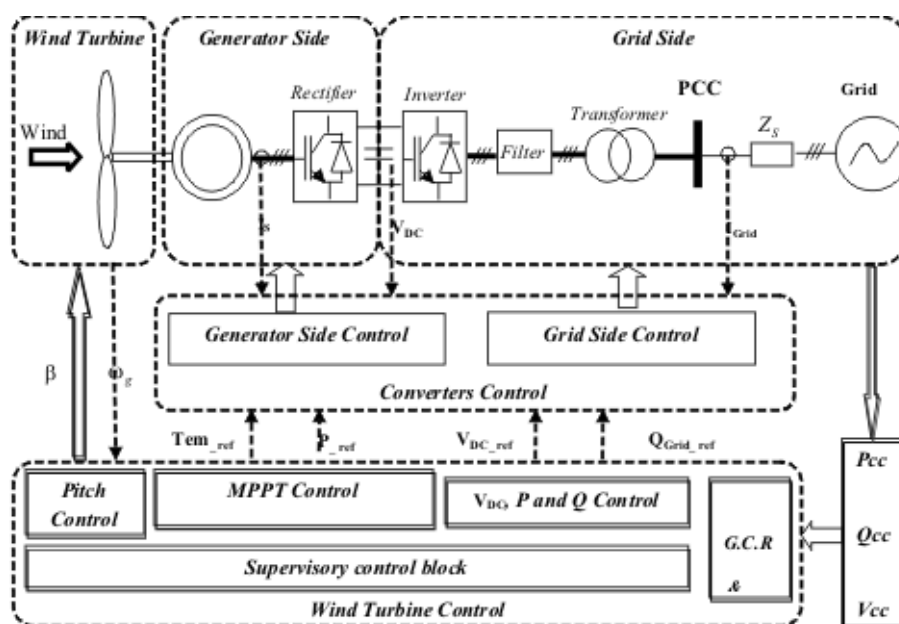


Figure 1: General control scheme of PMSG-WT

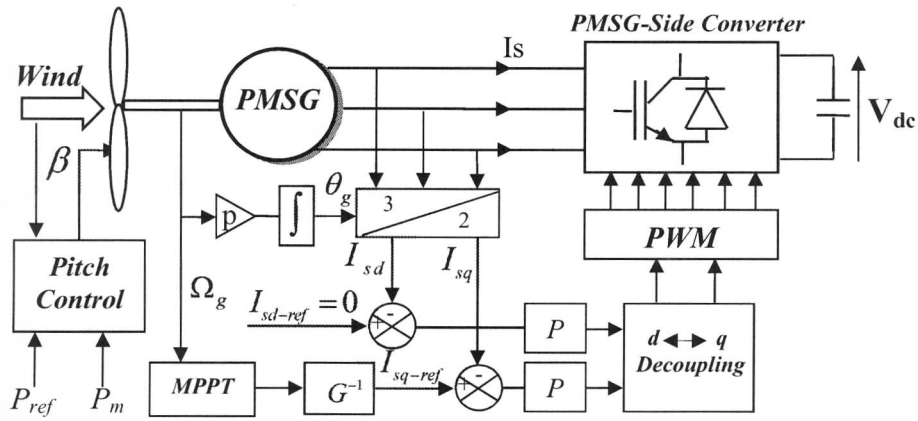


Figure 2: Block diagram of the field oriented control

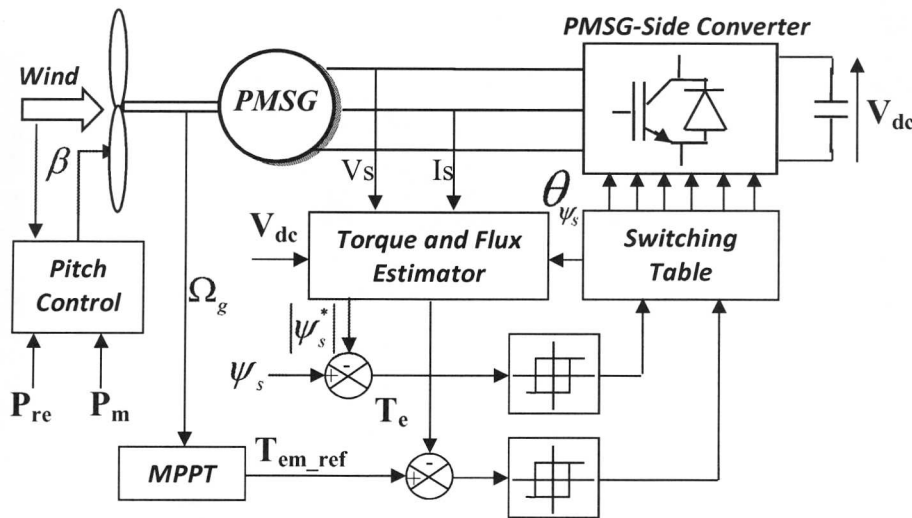


Figure 3: Block diagram of the direct torque control

other hand, DTC technique offers the fastest transient behaviour without overshoot (~9%). Table 1 shows a brief description of simulation results along with the characteristics of each control strategies.

Table.1: Control features and requirements for FOC and DTC control

Features	FOC	DTC
Switching Frequency	Constant $f = 2 \text{ kHz}$	Constant $f = 5 \text{ kHz}$
Modulation Technique	PWM	Hysteresis
Current THD	4.6%	11.2%
Tracking Error	0.83%	6.79%
Torque TWO	1.34%	1.03%
Cross-coupling Effect	Yes	No
Dynamic performance	Setting time ($< 112 \text{ ms}$)	Setting time ($< 82 \text{ ms}$)
	Rise time ($< 22 \text{ ms}$)	Rise time ($< 17 \text{ ms}$)
	Overshoot (~24%)	Overshoot (~9%)

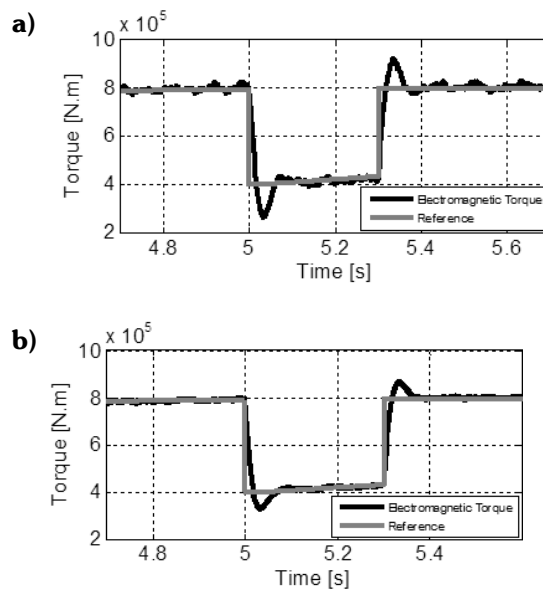


Figure 4: Simulation results versus the time-domain waveforms of the PMSG electromagnetic torque, during a load transient: a) FOC technique; b) DTC technique

4. Grid side converter control strategies

4.1 Voltage oriented control (VOC)

The grid side converter is mainly used to control active and reactive powers delivered to the grid, in order to keep the DC Link voltage constant, and to ensure the quality of the injected power. Voltage Oriented Control requires internal current control loops in the rotating dq frame and the elimination of the current cross coupling between the d and q components (Belhadj *et al.*, 2006; Woo Kim *et al.*, 2010). The connection to the grid is achieved through an LCL filter and a transformer. The Phased Locked Loop (PLL) gives an estimation of the angle of the grid voltage. In this way, an accurate synchronization between the inverter voltage and the voltage at the Point Common Coupling (PCC) is obtained. The PLL technique is detailed in Allagui *et al.*, (2013). The control of the DC-link voltage, active and reactive power delivered to the grid, and grid synchronization are shown in Figure 5.

4.2 Direct power control (DPC)

Conventional direct power control allows to directly controlling active and reactive powers using a switching table. It uses the same principle of DTC. Conventional DPC is characterized by the high ripple in grid currents which gives a poor power quality (Escobar *et al.*, 2003). In addition, the switching frequency is not controlled, which increase the difficulty for correct harmonic filter design. Consequently, conventional DPC is combined with SVM technique to obtain constant switching frequency and low current distortion (Malinowski *et al.*, 2004). The developed DPC for the grid-side converter is shown in Figure 6. In this figure, the unity power factor is obtained by setting the reactive power reference to zero.

4.3 Comparative study of DPC and VOC control

The steady-state is evaluated by means of current THD measurements, active and reactive power

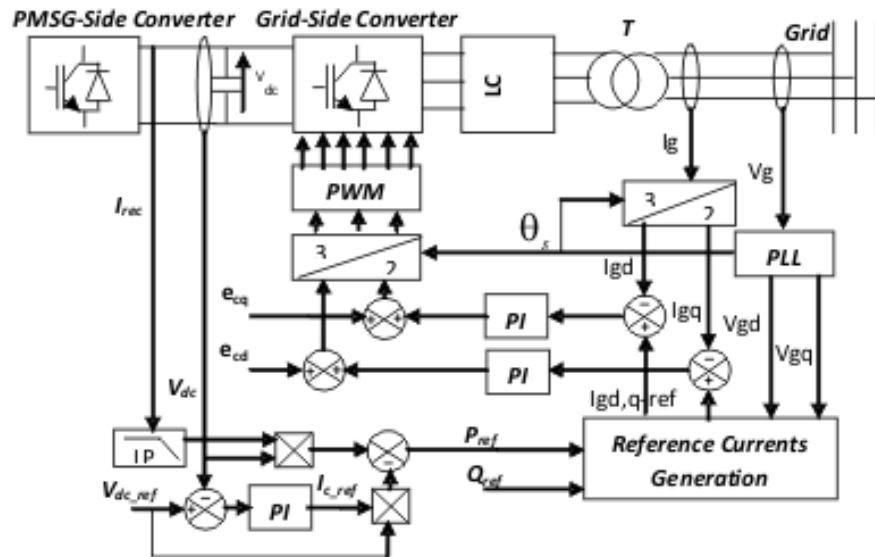


Figure 5: Block diagram of the voltage oriented control technique

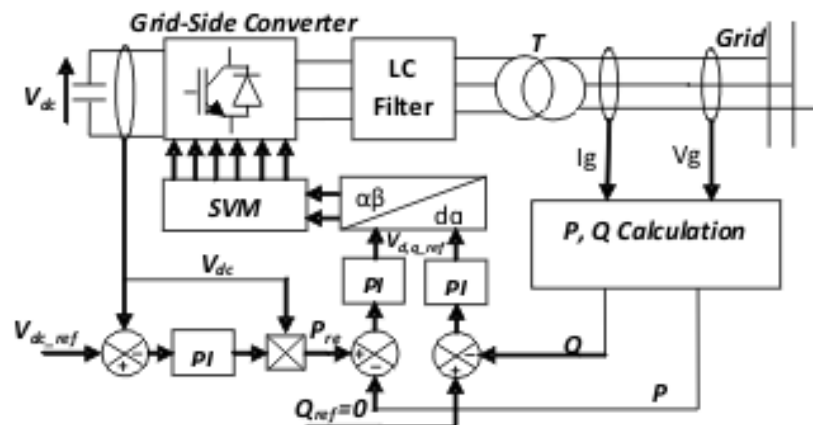


Figure 6: Block diagram of the direct power control technique

ripple values (ΔP , ΔQ) and some DC-link performance features as the voltage ripple ΔV_{DC} . On the other hand, the cross-coupling effect and the typical dynamic performance criterions as the settling time, rise time and overshoot are considered in the transient-state operation.

4.3.1 Steady-state performance

Figures 7 and 8 show the grid currents, spectrum analysis and power performance for the grid side converter, using both the VOC-type control strategy and the DPC techniques. As can be observed, the VOC control shows the best power quality (THD = 2.3%) and the minimum power ripple ($\Delta P = 8\%$, $\Delta Q = 9.2\%$). The DPC control leads to a dispersed harmonic spectrum with a large THD of around 9% with considerable power ripple values ($\Delta P = 17.6\%$, $\Delta Q = 19.4\%$).

According to the IEEE standards 519-1992 recommendation, the limit of harmonic distortions for distributed power systems connected to the grid should not exceed 5% (IEEE 519 Working Group, 1992). In this way, only VOC meets the grid connection requirements (GCR). On the other hand, the VOC strategy shows a small tracking error of around 0.32%, while the absolute tracking error reaches 4% in the DPC case. Furthermore, the voltage ripple in the DC-link capacitor is clearly smaller in the VOC ($\Delta V_{DC} = 5\%$) than the DPC strategy ($\Delta V_{DC} = 14\%$), see Figure 9.

4.3.2 Transient performances

Several simulations have been carried out in order to verify the behaviour of the proposed control algorithms during transients operation. These simulations involve the grid side converter configura-

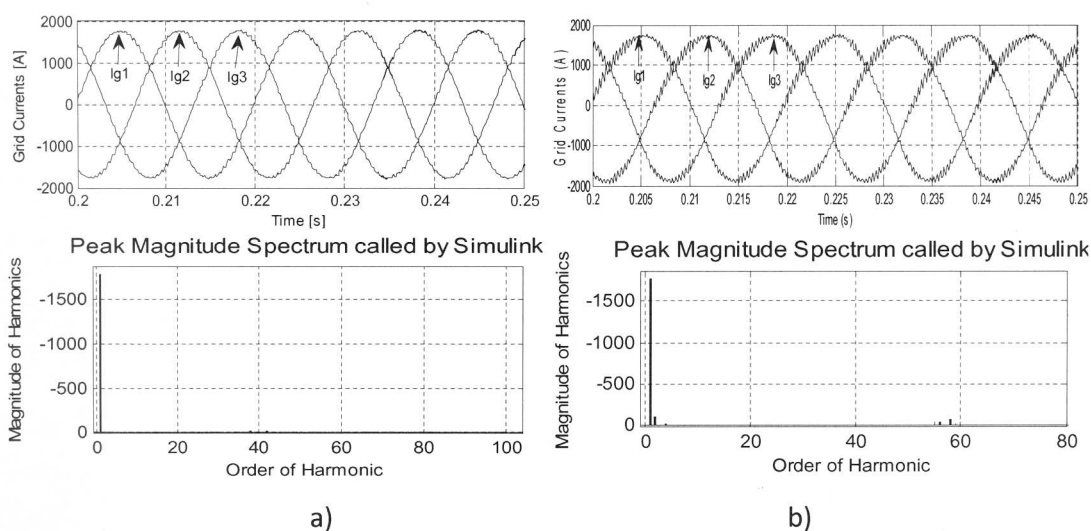


Figure 7: Grid currents and their spectrum analysis: a) VOC techniques b) DPC techniques

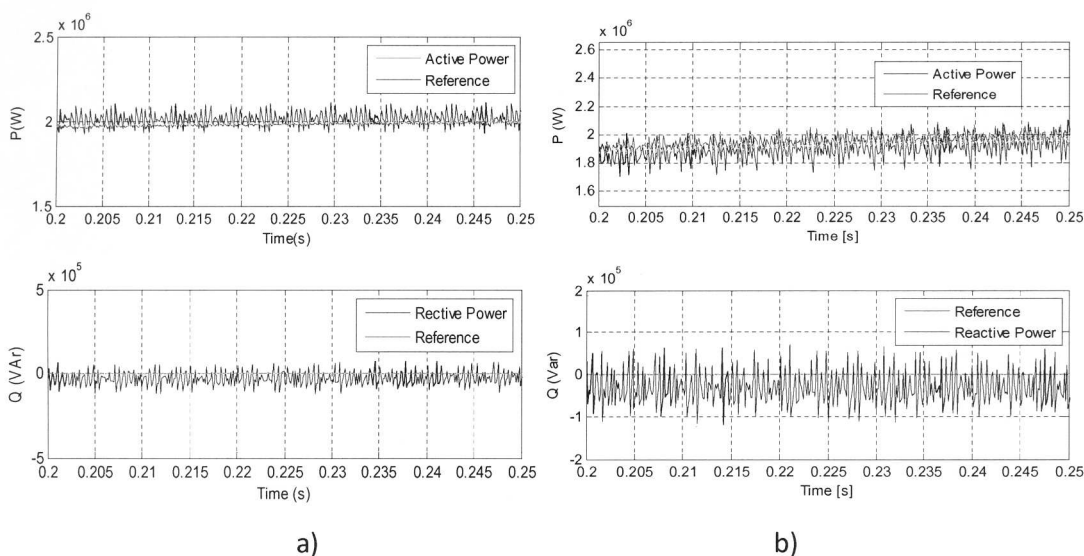


Figure 8: Active and reactive power behaviours: a) VOC techniques b) DPC techniques

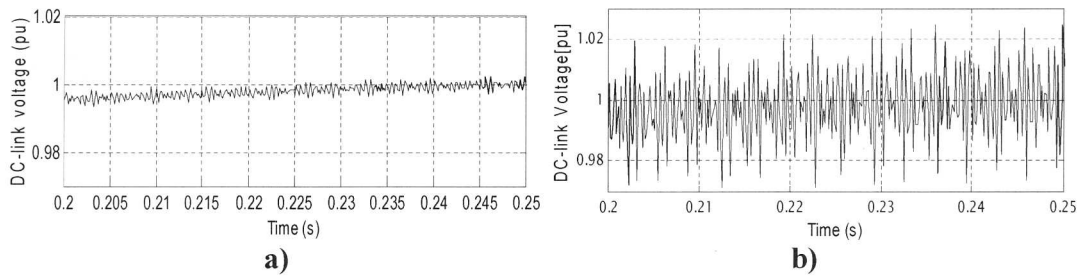


Figure 9: DC-link voltage: a) VOC techniques b) DPC techniques

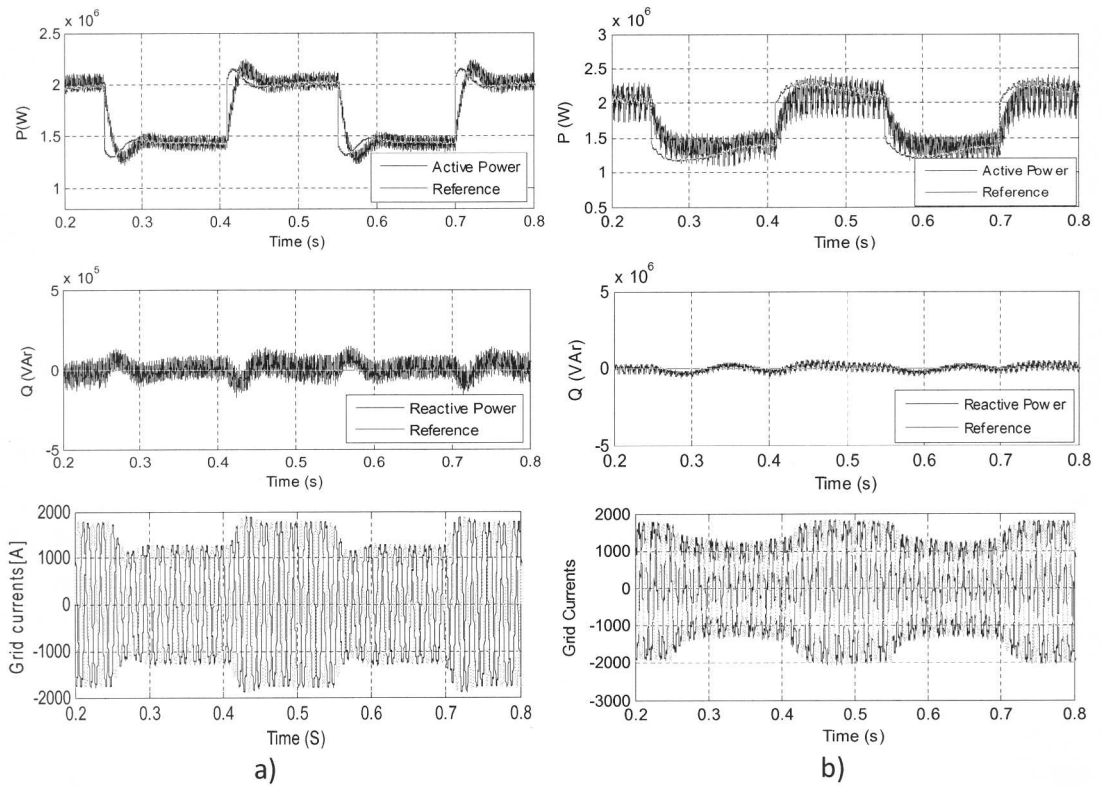


Figure 10: Instantaneous response during active and reactive power reference steps: a) VOC techniques b) DPC techniques

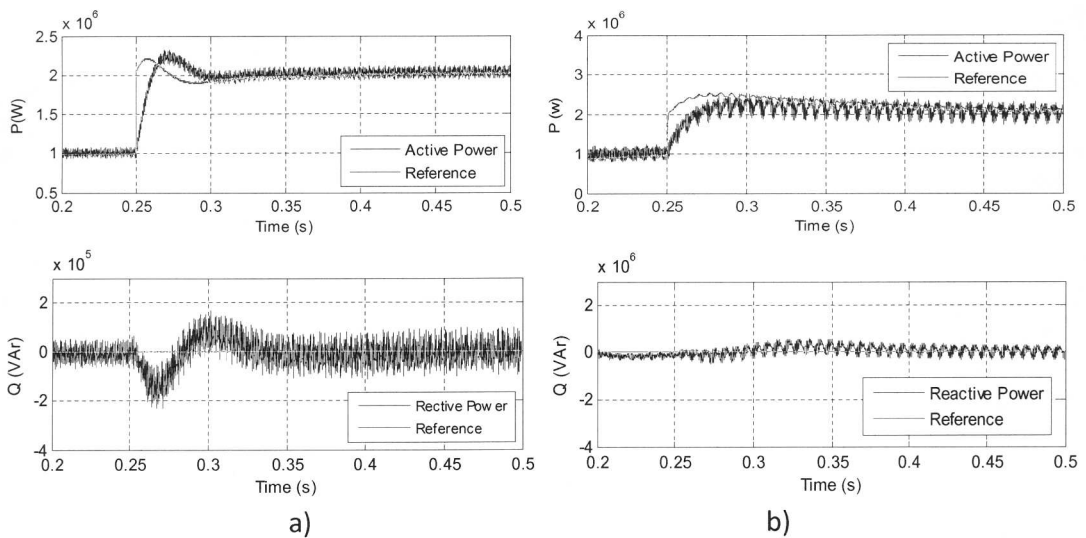


Figure 11: Active and reactive power transient behaviours: a) VOC techniques b) DPC techniques

tions with the VOC and DPC-based control strategies. Active-power reference steps from 1.4MW to 2MW have been applied (30% of nominal power). Note that reactive power steps will produce similar results in transients, so these cases are not evaluated. Figure 10 shows the instantaneous active and reactive power behaviour during active reference steps. As shown, the DPC technique is clearly faster than the VOC techniques in the power tracking task. The transient performance shows the expected behaviour in the VOC-based strategy (Figure 11).

To quantify the transient behaviour, a power band near 5% of the rated power is established. In this way, a setting time close to 60.6ms, a rise time below 17.2ms and a small overshoot of around 25% can be observed in the VOC-based configuration. Yet, the DPC needs a setting time below 44.8ms, with a rise time of around 13ms without overshoot (~5%) in power tracking requirements. Furthermore, there is no cross-coupling effect between active and reactive power in the DPC, whereas the VOC shows a substantial perturbation in the reactive power behaviour when active power changes are applied.

The steady-state simulations show the best power quality features and the smaller power-tracking error is obtained with VOC techniques. On the other hand, DPC -based strategies offer the fastest transient behaviour without overshoot and cross-coupling effect. Table 2 shows a brief description of the simulation results along with the characteristics and requirements of each control strategy. Consequently, it is concluded that combination of vector and direct control represents the best choice, depending on the desired performance trade-off.

5. Reactive power control supervisory
5.1 Low voltage ride through (LVRT) capabilities and voltage grid support

Currently, wind turbines should stay connected to the grid in the case of voltage dips (Lather *et al.*,

Table 2: Control features and requirements for VOC and DPC techniques

Features	VOC	DPC
Switching Frequency	f = 2 kHz Constant	f = 5 kHz Mean value
Modulation Technique	PWM	SVM
Current THD	2.3%	8.77%
Tracking Error	0.32%	4%
Power ripple	ΔP (8%) ΔQ (9.2%)	ΔP (17.6%) ΔQ (19.4%)
DC-link Ripple	ΔV_{DC} (5%)	ΔV_{DC} (14%)
Cross-coupling Effect	Yes	No
Dynamic Performance	Setting time (<60.6ms) Rise time (<17.2ms) Overshoot (~25%)	Setting time (<44.8ms) Rise time (<13.3ms) Overshoot (~5%)

2013). This is of particular importance to the TSOs, since wind farms disconnection could cause major loss of power generation and consequently, power system instability (Lov *et al.*, 2007; E.ON Netz GmbH, 2006). Grid connection requirements used in this paper are those defined by the TSO E.ON Netz and are presented in Figure 12 (Lov *et al.*, 2007). According to these requirements, wind farms should remain connected to the grid following voltage sag with a 100% magnitude during a minimal period of 150 ms. The Figure shows the limit above which turbines should not trip.

The purpose of the supervisory reactive power control presented in this section is to regulate the voltage at the specified PCC (Figure 13). To achieve this target, the Grid side converter must supply reactive current equivalent to 2% In per 1% Un voltage dip. Thus, the supervisory control block contains two control levels which are activated according to the dip magnitude:

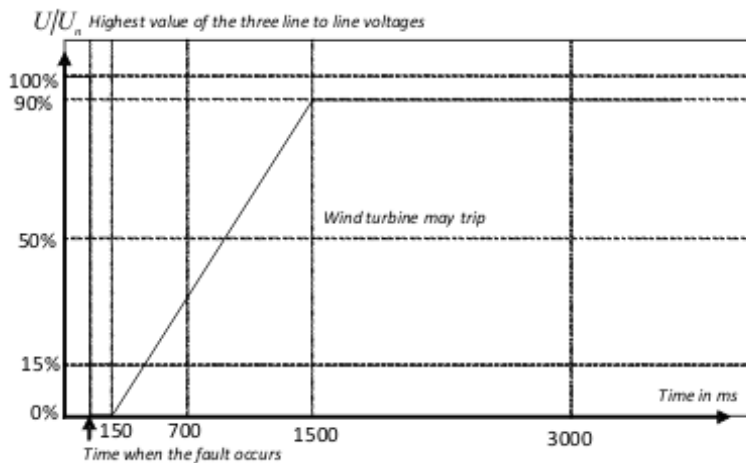


Figure 12: Voltage profile according to the requirements of LVRT capability through Lov *et al.*, (2007)

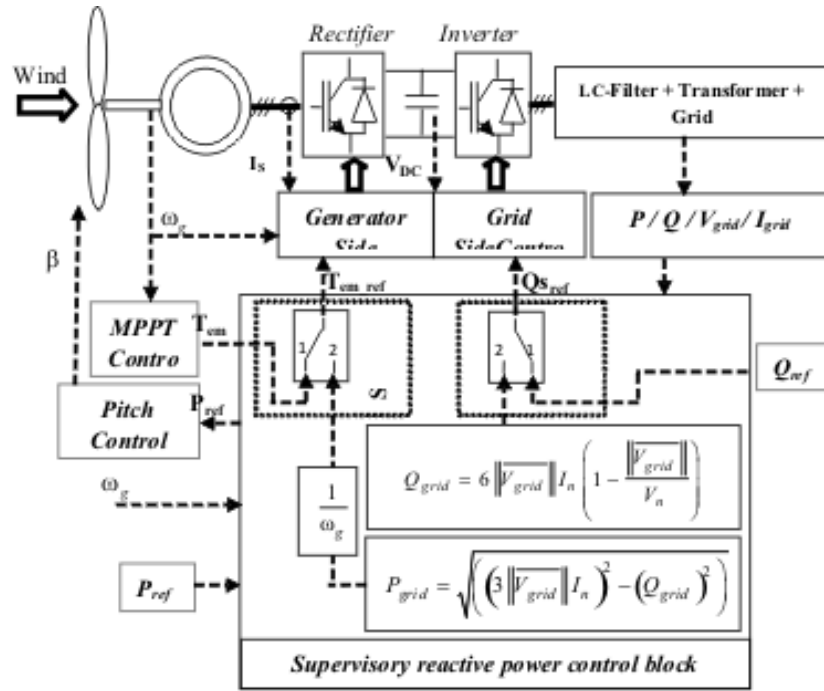


Figure 13: Schematic diagram of the reactive power supervisory

- *Level 1:* $\|V_{grid}\| \geq 50\%V_n$:
In this condition, the normal operating mode is activated. The torque reference T_{em_ref} is given by the MPPT algorithm and power production is optimized. Reactive power reference is fixed by the TSOs.
- *Level 2:* $\|V_{grid}\| \leq 50\%V_n$:
During faults, the wind turbine should supply reactive currents to the grid. In addition, grid currents should not exceed nominal ratings of power semiconductors. Therefore, reactive power reference Q_{grid} is calculated by:

$$Q_{grid} = 6 \|V_{grid}\| I_n \left(1 - \frac{\|V_{grid}\|}{V_n} \right) \quad (2)$$

Then, Q_{grid} is used to calculate active power reference P_{grid} given by (3):

$$P_{grid} = \sqrt{\left(\left(3 \|V_{grid}\| I_n \right)^2 - \left(Q_{grid} \right)^2 \right)} \quad (3)$$

The calculated power P_{grid} should be available at the output of the generator side converter. Therefore, when a voltage dip is detected, torque reference switches to another value given by (4):

$$T_{em-ref} = \frac{P_{grid}}{\omega_g} \quad (4)$$

5.2 Comparative study of DPC and VOC control

Figure 14 and 15 show the response of the control strategy to a symmetrical voltage dip. The dip magnitude is divided in two part; 45% then 70% of the rated voltage, as illustrated in Figure 15.

This result shows that DC-link voltage remains stable during the fault and the over-voltage does not exceed 10% of the rated value. For both control techniques; the wind turbine remains connected to the grid and supports the voltage by delivering reactive power, the grid currents are limited to the nominal value. After the fault, the active power is increased to the initial value with a gradient higher than 20% of the rated power per second, as required by the GCR. It is noticed that rotor speed is no longer controlled during the fault since torque reference is not taken from the MPPT algorithm. Finally, vector control technique (VOC) is characterized by a lower harmonic distortion THD and higher efficiency. On the other hand, DTC is less computational demanding and it gives a better dynamic response.

6. Conclusion

The synthesis and analysis of two different control strategies for PMSG-WT have been carried out. The results of this comparative study show that both control strategies can be used to control direct drive wind turbines. However, the best power quality features and the smaller power-tracking error are obtained with vector control techniques. On the other hand, direct control offers the better dynamic response without overshoot and cross-coupling effect.

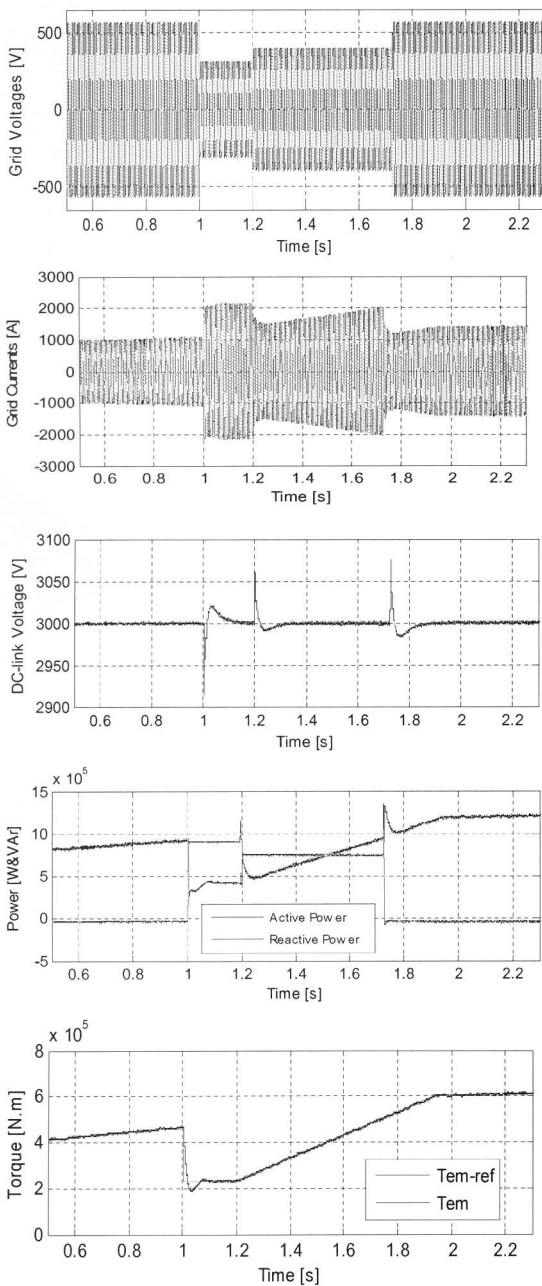


Figure 14: Wind turbine behaviour during a asymmetrical fault (type A), with the VOC techniques

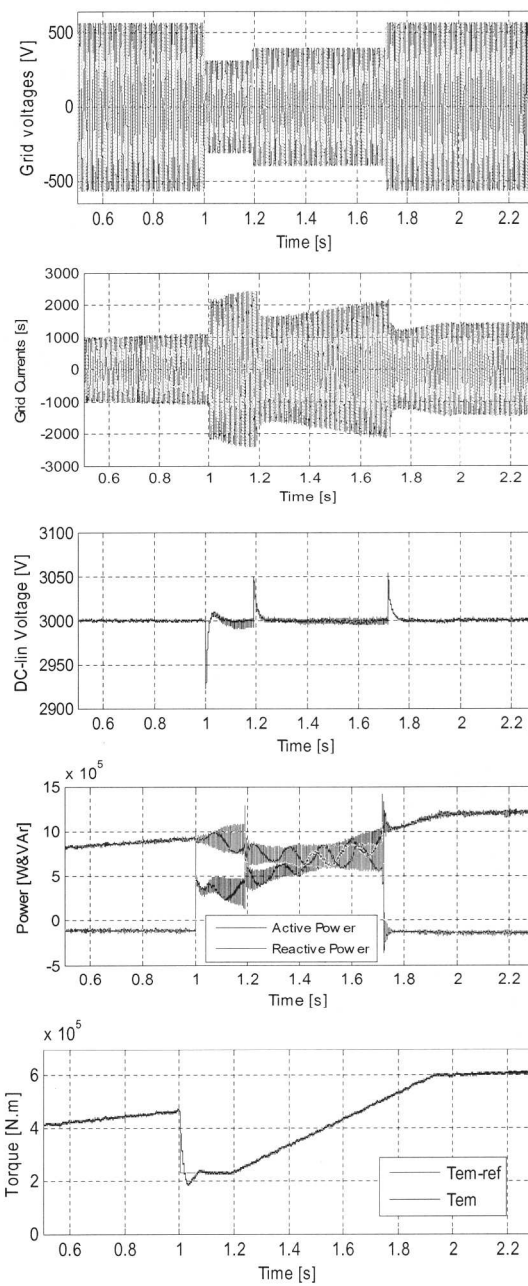


Figure 15: Wind turbine behaviour during a symmetrical fault (type A), with the DPC techniques

According to the simulation results, the wind turbine does not trip during a grid fault. In addition it delivers reactive power to support the grid voltage. Thus, supervisor performances are in accordance with the GCR for both control strategies. We conclude that the vector control is better as adapted, and the responses with the direct control are faster.

Appendix: See overleaf

Acknowledgment

This work was supported by the Tunisian Ministry of High Education, Research and Technology.

References

Akhmatov, V., (2005). Modelling and Ride-through Capabilities of Variable Speed Wind Turbines With Permanent Magnet Generators, Wiley Interscience, Vol. 1, pp. 1-14.

Allagui, M., Hasnaoui, O.B.K., and Belhadj, J., (2013). Exploitation of pitch control to improve the integration of a direct drive wind turbine to the grid, *Journal of Electrical Systems*, 9(2), pp. 179-190.

Belhadj, J., and Xavier, R., (2006). Investigation of Different Methods to Control a Small Variable-Speed Wind Turbine With PMSM Drives, *ASME Journal of Energy Resources Technology*, 129(3), pp. 200-213. doi:10.1115/1.2748813

Bin Wu, Yongqiang Lang, Navid Zargari, Samir Kouro, (2011). Power Conversion and Control of Wind

- Energy Systems John Wiley & Sons.
- Carlsson, A., (1998). The back-to-back converter, Thesis, Lund Institute of Technology, Lund, Sweden.
- E.ON Netz GmbH, (2006). Netzanschlussregeln für Hoch- und Höchstspannung, Bayreuth.
- Escobar, G., Stankovic, A.M., Carrasco, J.M., Galvan, E., and Ortega, R., (2003). Analysis and design of direct power control (DPC) for a three phase synchronous rectifier via output regulation subspaces, *IEEE Transactions on Power Electronics*, 18(3), pp. 823-830.
- Gabriele, M., (2008). Variable Speed Wind Turbines - Modelling, Control, and Impact on Power Systems, PhD thesis, Department of Renewable Energies at Darmstadt Technical University (Germany).
- Heier, S., (2006). Grid integration of wind energy conversion systems, John Wiley & Sons Ltd, 2nd ed., Chichester, UK.
- IEEE 519 Working Group, (1992). IEEE Recommended Practices and Requirements for Harmonic Control in Electrical Power Systems, IEEE STD 519-1992.
- Lather, J.S., Dhillon, S.S. and Marwaha, S., (2013). Modern Control Aspects In doubly fed Induction Generator Based Power Systems: A Review, *International Journal of Advanced Research in Electrical, Electronics and Instrumentation Engineering* Vol. 2, Issue 6, pp.2149-2161.
- Lov, F., Daniela Hansen, A., Sørensen, P., and Antonio Cutululis, N., (2007). Mapping of grid faults and grid codes, Technical University of Denmark, Vol: Risø-R-1617(EN), Publisher: Risø National Laboratory, Roskilde Denmark.
- Malinowski, M., Jasinski, M., and Kazmierkowski, M. P., (2004). Simple direct power control of three phase PWM rectifier using space-vector modulation (DPC-SVM), *IEEE Transactions on Industrial Electronics*, 51(2), pp. 447-454.
- Muni Prakash, T., and Shakeer Ahhamad, SK., (2012). Direct torque control for doubly fed induction machine-based wind turbines under voltages dips and without crowbar protection, *International Journal of Electrical and Electronics Engineering*, Vol-1 Iss-4, pp. 52-54.
- Pena, R., Clare, J.C., Asher, G.M., (1996). Doubly-fed induction generator using back-to-back PWM converters and its application to variable speed wind energy generation, *IEEE proceedings on electronic power application*, 143(3), 231-241.
- Rahman, M. F., Zhong, L., Haque, E., and Rahman, M. A., (2003). A Direct Torque-Controlled Interior Permanent-Magnet Synchronous Motor Drive Without a Speed Sensor, *IEEE Trans. Energy conversion*, 18(1).
- The European Wind Energy Association, (2010). Gwec – Table and Statistics 2009. Available online: <http://www.ewea.org>.
- Woo Kim, H., Kim, Sung-Soo., Hee-Sang, Ko., (2010). Modelling and control of PMSG-based variable-speed wind turbine, *Electric Power Systems Research*, Vol. 80, 46-52.

Received 3 November 2013; revised 16 May 2014

Appendix: Wind turbine, PMSG side and grid side parameters

Wind Turbine Parameters	PMSG side parameters	Grid side parameters
$P = 2MW$	$P_{nom} = 2.02MW$	$S = 2MW$
$N_m = 24rpm$	$U_{nom} = 1.75kV$	$U_{dc} = 3kV$
$J_{tot} = 6.2 \cdot 10^6 kg.m^2$	$I_s = 660A$	$C_{dc} = 20mF$
$D = 75m$	$r_s = 32m\Omega$	$R_g = 0.3m\Omega$
3 Blades	$L_{sd} = 2.7mH$	$L_g = 0.01mH$
Variable Speed	$L_{sq} = 1.7mH$	$C_f = 35\mu F$
Collective Pitch	$\phi_v = 18.6wb$	
	$p = 32$	